Inorg. Chem. **2006**, *45*, 10764–10773

Syntheses, Structures, and Magnetic Properties of Mononuclear Cu^{II} and Tetranuclear $Cu^{II}_3M^{II}$ (M = Cu, Co, or Mn) Compounds Derived from *N,N′*-Ethylenebis(3-ethoxysalicylaldimine): Cocrystallization Due to Potential Encapsulation of Water

Malabika Nayak,[†] Rajesh Koner,[†] Hsin-Huang Lin,[‡] Ulrich Flörke,[§] Ho-Hsiang Wei,*[,‡] and Sasankasekhar Mohanta*[,†]

Department of Chemistry, University of Calcutta, 92 A. P. C. Ray Road, Kolkata 700 009, India, Department of Chemistry, Tamkang University, Tamsui, Taiwan 25137, and Anorganische and Analytische Chemie, Universität Paderborn, D-33098 Paderborn, Germany

Received June 12, 2006

Syntheses, structures, and magnetic properties of one mononuclear inclusion compound $[Cu^{II}L^1{\subset}(H_2O)]$ (**1**) and three tetrametal systems of the composition $[\{Cu^{II}L^1\}_2\{Cu^{II}L^1M^{II}(H_2O)_3\}](ClO_4)_2$ (M = Cu (**2**), M = Co (**3**), M = Mn (**4**)) derived from the hexadentate Schiff base compartmental ligand *N,N′*-ethylenebis(3-ethoxysalicylaldimine) (H_2L^1) have been described. Compounds **1** and **2** crystallize in orthorhombic *Pbcn* and monoclinic $P2_1/c$ systems, respectively, and the space group of the isomorphous compounds **3** and **4** is monoclinic *C*2/*c*. The water molecule in **1** is encapsulated in the vacant O_4 compartment because of the hydrogen bonding interactions with the ether and phenolate oxygens, resulting in the formation of an inclusion product. The structures of **2**–**4** consist of the $[Cu^{II}L^1M^{II}(H_2O)_3]^{2+}$ cation and two mononuclear $[Cu^{II}L^1]$ moieties. In the dinuclear $[Cu^{II}L^1M^{II}(H_2O)_3]^{2+}$ cation, the metal centers are doubly bridged by the two phenolate oxygens. The second metal center, M^{II} (Cu in **2**, Co in **3**, and Mn in **4**), in the $[Cu^{II}L^1M^{II}(H_2O)_3]^{2+}$ cation is pentacoordinated by the two phenoxo oxygens and three water molecules. Two of these three coordinated water molecules interact, similar to that in **1**, with two mononuclear $[Cu^{II}L^1]$ moieties, resulting in the formation of the tetrametal $[\{Cu^{II}L^1\}_2\{Cu^{II}L^1M^{II}(H_2O)_3\}]^{2+}$ system that consists of the cocrystallized dinuclear (one) and mononuclear (two) moieties. Evidently, the cocrystallization observed in **2**–**4** is related to the tendency of a water molecule to be encapsulated in the vacant O_4 compartment of the mononuclear $[Cu^{II}L^1]$ species. In the case of **2**, there are two independent $[Cu^{II}L^1Cu^{II}(H_2O)_3]^{2+}$ units. The τ ($(\beta - \alpha)/60$, where β and α are the largest and second largest bond angles, respectively) values in the pentacoordinated environment of the two copper(II) centers in **2** are 0.04 and 0.37, indicating almost ideal and appreciably distorted square pyramidal geometry, respectively. In contrast, the τ values (0.54 for **3** and 0.49 for **4**) indicate that the coordination geometry around the cobalt(II) and manganese(II) centers in **3** and **4** is intermediate between square pyramidal and trigonal bipyramidal. The variable-temperature (2–300 K) magnetic susceptibilities of compounds **2**–**4** have been measured. The magnetic data have been analyzed in the model of one exchange-coupled dinuclear $Cu^{II}M^{II}$ moiety and two noninteracting Cu^{II} centers. In all three cases, the metal ions in the dinuclear core are coupled by a weak antiferromagnetic interaction ($J = -17.4$ cm^{-1}, -8 cm^{-1}, and -14 cm^{-1} for **2**, **3**, and **4**, respectively). The observation of a weak interaction has been explained in terms of the structural parameters and symmetry of the magnetic orbitals.

Introduction

The successful development of crystal engineering strategies relies first on developing, understanding, and rationalizating intermolecular interactions in the context of crystal packing, followed by the subsequent utilization and exploitation of this understanding in the design of new solids with predictable structural properties.[1,2] Intermolecular interactions between the same molecules result in the generation of di- and oligomers as well as extended networks.[1,2] Similarly, the attractive forces between different moieties may result in the formation of multicomponent crystals, which are

* To whom correspondence should be addressed. E-mail: sm_cu_chem@yahoo.co.in (S.M.), tkwei@mail.tku.edu.tw (H.-H.W.). Fax: 91-33-23519755 (S.M.), 886-2-26209924 (H.-H.W.).
[†] University of Calcutta.
[‡] Tamkang University.
[§] Universität Paderborn.

10.1021/ic061049u CCC: $33.50
Published on Web 11/17/2006

known as cocrystals, of varying dimensionality.[2e−h,3−6] Definitely, cocrystallization of two different molecules is a possible way of intentionally influencing the position of molecules in a crystal lattice and allows for the investigation of newly generated macroscopic properties. Designed syntheses of cocrystals have attracted much attention in recent years for the understanding and exploitation of intermolecular interactions as well as for their importance as pharmaceuticals, nonlinear optical materials, and charge-transfer solids.[2g,3a,4a,5c]

The reported cocrystals are dominated by organic systems,[2e−h,3,4] the majority of which, in turn, are acid−base compounds.[2e−h,4] There are also several examples of inorganic−organic cocrystals.[5] However, cocrystals containing only the metal complexes are very rare.[6] Again, although the design of the components as well as the understanding of the reason of cocrystallization in organic cocrystals is well explored in terms of the noncovalent interactions, not only is the cocrystallization of the metal compounds accidental but also the governing factors of this structural phenomenon therein are difficult to understand. Clearly, the design of metal compounds that can exhibit inherent cocrystallization behavior remains a challenging task.

It is well-known that the excellent hydrogen bonding ability of water plays a crucial role in stabilizing the solid-state structure of numerous crystal hydrates. In some of the host−guest compounds or inclusion compounds, water can be encapsulated and behaves as a guest by forming hydrogen bonds with the electron donor centers of the host molecules such as crown ethers,[7] molecular tweezers,[8] and metal compounds containing a vacant compartment.[9] However, the role of water for potential cocrystallization of metal compounds or any other type of system is not well-known.

A number of mono- and dinuclear compounds have been derived previously from the compartmental Schiff base ligands obtained on condensation of 3-methoxy/ethoxysalicylaldehyde with diamines.[9−11] In the mononuclear compounds, a 3d metal ion occupies the N_2O_2 cavity. In some of the mononuclear compounds of nickel(II) and oxovanadium(IV), one water molecule is encapsulated in the O_4 compartment, resulting in the formation of an inclusion product.[9] Again, there are also a few nonhydrated compounds of the same metal ions derived from the similar ligands.[10b−d] There is only one structurally characterized mononuclear copper(II) compound, $[Cu^{II}(L)(H_2O)]$ (H_2L = *N*,*N*′-ethylenebis(3-methoxysalicylaldimine), derived from this class of compartmental ligands.[10a] In this compound, the water molecule is coordinated to the square pyramidal metal center. Clearly, the encapsulation of a water molecule in the vacant O_4 cavity is not a general phenomenon of this type of mononuclear compound but depends on the subtle effect characteristic of a particular compound. The dinuclear

(1) (a) Sauvage, J.-P., Ed. *Transition Metals in Supramolecular Chemistry*; Perspectives in Supramolecular Chemistry 5; Wiley: London, 1999. (b) Desiraju, G. R., Ed. *The Crystal as a Supramolecular Entity*; Perspectives in Supramolecular Chemistry 2; Wiley: London, 1996. (c) Braga, D.; Grepioni, F.; Orpen, A. G. *Crystal Engineering*: *From Molecules and Crystals to Materials*; Kluwer Academic Publishers: Dordrecht, The Netherlands, 1999. (d) Moulton, B.; Zaworotko, M. J. *Chem. Rev.* **2001**, *101*, 1629. (e) Blake, A. J.; Champness, N. R.; Hubberstey, P.; Withersby, M. A.; Schröder, M. *Coord. Chem. Rev.* **1999**, *183*, 117.

(2) (a) Maggard, P. A.; Kopf, A. L.; Stern, C. L.; Poeppelmeier, K. R.; Ok, K. M.; Halasyamani, P. S. *Inorg. Chem.* **2002**, *41*, 4852. (b) Maggard, P. A.; Stern, C. L.; Poeppelmeier, K. R. *J. Am. Chem. Soc.* **2001**, *123*, 7742. (c) Atwood, J. L.; Barbour, L. J.; Ness, T. J.; Raston C. L.; Raston, P. L. *J. Am. Chem. Soc.* **2001**, *123*, 7192. (d) Dalgarno, S. J.; Atwood, J. L.; Raston, C. L. *Cryst. Growth Des.* **2006**, *6*, 174. (e) Koshima, H.; Nagano, M.; Asahi, T. *J. Am. Chem. Soc.* **2005**, *127*, 2455. (f) Childs, S. L.; Chyall, L. J.; Dunlap, J. T.; Smolenskaya, V. N.; Stahly, B. C.; Stahly, G. P. *J. Am. Chem. Soc.* **2004**, *126*, 13335. (g) Remenar, J. F.; Morissette, S. L.; Peterson, M. L.; Moulton, B.; MacPhee, J. M.; Guzman, H. R.; Almarsson, O. *J. Am. Chem. Soc.* **2003**, *125*, 8456. (h) Zhang, X.-L.; Chen, X.-M. *Cryst. Growth Des.* **2005**, *5*, 617. (i) Koner, R.; Nayak, M.; Ferguson, G.; Low, J. N.; Glidewell, C.; Misra, P.; Mohanta, S. *Cryst. Eng. Commun.* **2005**, *7*, 129. (j) Nayak, M.; Koner, R.; Stoeckli-Evans, H.; Mohanta, S. *Cryst. Growth Des.* **2005**, *5*, 1907. (k) Lin, H.-H.; Mohanta, S.; Lee, C.-J.; Wei, H.-H. *Inorg. Chem.* **2003**, *42*, 1584. (l) Dutta, B.; Adhikary, B.; Bag, P.; Flörke, U.; Nag, K. *J. Chem. Soc., Dalton Trans.* **2002**, 2760. (m) Eringathodi, S.; Agnihotri, P.; Ganguly, B.; Bhatt, P.; Subramanian, P. S.; Paul, P.; Ghosh, P. K. *Chem.*−*Eur. J.* **2005**, 2198.

(3) (a) Keyes, T. E.; Forster, R. J.; Bond, A. M.; Miao, W. *J. Am. Chem. Soc.* **2001**, *123*, 2877. (b) Geiser, U.; Kumar, S. K.; Savall, B. M.; Harried, S. S.; Carlson, K. D.; Mobley, P. R.; Wang, H.-H.; Williams, J. M.; Botto, R. E. *Chem. Mater.* **1992**, *4*, 1077. **(c)** Olenik, B.; Boese, R.; Sustmann, R. *Cryst. Growth Des.* **2003**, *3*, 175. (d) Pan, F.; Wong, M. S.; Gramlich, V.; Bosshard, C.; Gunter, P. *J. Am. Chem. Soc.* **1996**, *118*, 6315.

(4) (a) Koshima, H.; Miyamoto, H.; Yagi, I.; Uosaki, K. *Cryst. Growth Des.* **2004**, *4*, 807. (b) Ohba, S.; Hosomi, H.; Ito, Y. *J. Am. Chem. Soc.* **2001**, *123*, 6349. (c) Loehlin, J. H.; Etter, M. C.; Gendreau, C.; Erika Cervasio, E. *Chem. Mater.* **1994**, *6*, 1218. (d) Bhogala, B. R.; Nangia, A. *Cryst. Growth Des.* **2003**, *3*, 547.

(5) (a) Lee, H. M.; Olmstead, M. M.; Gross, G. G.; Balch, A. L. *Cryst. Growth Des.* **2003**, *3*, 691. (b) Olmstead, M. M.; Wei, P.; Ginwalla, A. S.; Balch, A. L. *Inorg. Chem.* **2000**, *39*, 4555. (c) Le Magueres, P.; Hubig, S. M.; Lindeman, S. V.; Veya, P.; Kochi, J. K. *J. Am. Chem. Soc.* **2000**, *122*, 10073. (d) Ara, I.; Fornies, J.; Gomez, J.; Lalinde, E.; Moreno, M. T. *Organometallics* **2000**, *19*, 3137. (e) Wiechert, D.; Mootz, D.; Dahlems, T. *J. Am. Chem. Soc.* **1997**, *119*, 12665. (f) Koner, R.; Drew, M. G. B.; Figuerola, A.; Diaz, C.; Mohanta, S. *Inorg. Chim. Acta* **2005**, *358*, 3041.

(6) (a) Chou, C.-C.; Su, C.-C.; Tsai, H.-L.; Lii, K.-H. *Inorg. Chem.* **2005**, *44*, 628. (b) Palaniandavar, M.; Butcher, R. J.; Addison, A. W. *Inorg. Chem.* **1996**, *35*, 467. (c) Holz, R. C.; Thompson, L. C. *Inorg. Chem.* **1993**, *32*, 5251. (d) Jones, P.; Vagg, R. S.; Williams, P. A. *Inorg. Chem.* **1984**, *23*, 4110. (e) Evans, W. J.; Boyle, T. J.; Ziller, J. W. *Inorg. Chem.* **1992**, *31*, 1120.

(7) (a) Atwood, J. L., Devies, J. E. D., MacNicol, D. D., Eds. *Inclusion Compounds*; Academic Press: London, 1984. (b) Atwood, J. L., Devies, J. E. D., MacNicol, D. D., Vogtle, F., Lehn, J. M., Gokel, G. W., Eds. *Comprehensive Supramolecular Chemistry*; Pergamon Press: Exeter, U.K., 1996; Vol. 1. (c) Schneider, H. J.; Guetters, D.; Schneider, U. *J. Am. Chem. Soc.* **1988**, *110*, 6449. (d) Newkome, G. R.; Taylor, H. C. R.; Fronczek, F. R.; Delord, T. J.; Kohli, D. K.; Voegtle, F. *J. Am. Chem. Soc.* **1981**, *103*, 7376.

(8) Meyer, S.; Louis, R.; Metz, B.; Agnus, Y.; Varnek, A.; Gross, M. *New J. Chem.* **2000**, *24*, 371.

(9) (a) Hoshina, G.; Tsuchimoto, M.; Ohba, S. *Bull. Chem. Soc. Jpn.* **2000**, *73*, 369. (b) Cunningham, D.; Gallagher, J. F.; Higgins, T.; McArdle, P.; McGinley, J.; O'Gara, M. *J. Chem. Soc., Dalton Trans.* **1993**, 2183. (c) Zamian, J. R.; Dockal, E. R.; Castellano, G.; Oliva, G. *Polyhedron* **1995**, *14*, 2411.

(10) (a) Oleksyn, B. *Hang. Diff. Conf.* **1976**, *8*, 19. (b) Cashin, B.; Cunningham, D.; Daly, P.; McArdle, P.; Munroe, M.; Ni Chonchubhair, N. *Inorg. Chem.* **2002**, *41*, 773. (c) Hoshina, G.; Tsuchimoto, M.; Ohba, S. *Acta Crystallogr. C* **1999**, *55*, 1812. (d) Schmidt, H.; Bashirpoor, M.; Rehder, D. *J. Chem. Soc., Dalton Trans.* **1996**, 3865.

(11) (a) Winpenny, R. E. P. *Chem. Soc. Rev.* **1998**, 447. (b) Sakamoto, M.; Manseki, K.; Ōkawa, H. *Coord. Chem. Rev.* **2001**, *219*−*221*, 379. (c) Koner, R.; Lin, H.-H.; Wei, H.-H.; Mohanta, S. *Inorg. Chem.* **2005**, *44*, 3524. (d) Koner, R.; Lee, G.-H.; Wang, Y.; Wei, H.-H.; Mohanta, S. *Eur. J. Inorg. Chem.* **2005**, 1500. (e) Mohanta, S.; Lin, H.-H.; Lee, C.-J.; Wei, H.-H. *Inorg. Chem. Commun.* **2002**, *5*, 585. (f) Novitchi, G.; Shova, S.; Caneschi, A.; Costes, J.-P.; Gdaniec, M.; Stanica, N. *J. Chem. Soc., Dalton Trans.* **2004**, 1194. (g) Costes, J.-P.; Dahan, F.; Novitchi, G.; Arion, V.; Shova, S.; Lipkowski, J. *Eur. J. Inorg. Chem.* **2004**, 1530. (h) Costes, J.-P.; Dahan, F.; Dupuis, A.; Laurent, J.-P. *Inorg. Chem.* **2000**, *39*, 169.

Chart 1. Chemical Structure of H_2L^1

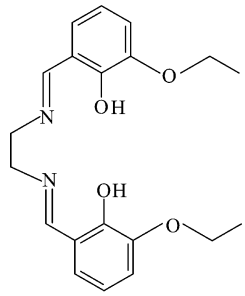

H_2L^1

compounds derived from the above-mentioned compartmental ligands are dominated by the 3d−4f systems.[11] However, the homo- and heterodinuclear 3d−3d compounds derived from this type of ligand system are not well-known. In the 3d−4f compounds, due to the oxophilicity of the lanthanide ions, all four oxygen atoms coordinate to the 4f centers. In contrast, as the ether oxygens are not a suitable coordinating center to the 3d metal ion and as the ionic radius of the 3d metal ion is smaller, it is expected that the ether oxygens will not coordinate to the second metal center in the 3d−3d compounds. In that case, there is a possibility that the remaining coordination positions of the second metal center will be satisfied by a number of water (or other solvent) molecules. Therefore, if the 3d−3d compounds in this type of ligand environment can be stabilized, a new type of dinuclear core will be generated, which, in turn, may shed light upon the spin exchange properties between the 3d metal ions.[12]

The present investigation concerns the mononuclear copper(II) compound, $[Cu^{II}L^1\subset(H_2O)]$ (**1**); (H_2L^1 = *N*,*N*′-ethylenebis(3-ethoxysalicylaldimine); Chart 1), and the products obtained on reaction of **1** with the perchlorate salts of copper(II), cobalt(II), and manganese(II). We are particularly interested in checking the possibility of the inclusion of water in the mononuclear copper(II) compound as well as in exploring the 3d−3d compounds in this ligand environment. Interestingly, the reaction of **1** with $M(ClO_4)_2\cdot 6H_2O$ results in the formation of the self-assembled tetranuclear systems, $[\{Cu^{II}L^1\}_2\{Cu^{II}L^1M^{II}(H_2O)_3\}](ClO_4)_2$ (M = Cu (**2**), M = Co (**3**), M = Mn (**4**)), consisting of the cocrystal of the dinuclear $[Cu^{II}L^1M^{II}(H_2O)_3]^{2+}$ cation and two mononuclear $[Cu^{II}L^1]$ species. The syntheses, characterization, structures, and magnetic properties of **1**−**4** are described in the present study.

Experimental Section

Materials and Physical Measurements. All the reagents and solvents were purchased from the commercial sources and used as received. The Schiff base ligand H_2L^1 was prepared according to the reported method.[11c] Elemental (C, H, and N) analyses were performed on a Perkin-Elmer 2400 II analyzer. IR spectra were recorded in the region 400−4000 cm^{-1} on a Perkin-Elmer RXIFT spectrophotometer with samples as KBr disks. Magnetic susceptibility measurements of **1** at 300 K were carried out with a magnetic susceptibility balance, Sherwood Scientific Co., U.K. Variable-temperature (5−300 K) magnetic susceptibility measurements under a fixed field strength of 1 T were carried out with a Quantum Design MPMS SQUID magnetometer. Diamagnetic corrections were estimated from the Pascal constants.[13]

Syntheses. $[Cu^{II}L^1\subset(H_2O)]$ (1). To a stirred suspension of the ligand H_2L^1 (1.78 g, 5 mmol) in methanol (15 mL) was added dropwise an aqueous solution (5 mL) of $Cu(OAc)_2\cdot H_2O$ (1.0 g, 5 mmol). During the addition, a brown product began to deposit. After stirring the mixture for 0.5 h, the brown solid was collected by filtration. Recrystallization of the product from dimethylformamide yielded diffraction quality crystals. Yield: 1.962 g (90%). Anal. Calcd for $C_{20}H_{24}N_2O_5Cu$: C, 55.10; H, 5.55; N, 6.43. Found: C, 55.20; H, 5.47; N, 6.48. IR (cm^{-1}, KBr): $\nu_{as}(H_2O)$, 3568m; $\nu_s(H_2O)$, 3518m; ν(C═N), 1620vs; $\delta(H_2O)$, 1545w; ν(C−OEt), 1246m. μ_{eff} = 1.78 BM (bohr magneton).

$[\{Cu^{II}L^1\}_2\{Cu^{II}L^1Cu^{II}(H_2O)_3\}](ClO_4)_2$ (2). To a suspension of **1** (0.218 g, 0.5 mmol) in methanol (15 mL) was added dropwise with stirring a methanol solution (5 mL) of copper(II) perchlorate hexahydrate (0.186 g, 0.5 mmol). Immediately, a green solution formed, which was filtered after 0.5 h to remove any suspended particles. The filtrate was then kept at room temperature for slow evaporation. After a few days, diffraction quality brown crystals that deposited were collected and washed with cold methanol. Yield: 0.209 g (80%). Anal. Calcd for $C_{60}H_{72}N_6O_{23}Cl_2Cu_4$: C, 45.89; H, 4.62; N, 5.35. Found: C, 45.67; H, 4.63; N, 5.27. IR (cm^{-1}, KBr): $\nu(H_2O)$, 3339w; ν(C═N), 1625s; $\nu(ClO_4)$, 1088vs, 620w.

$[\{Cu^{II}L^1\}_2\{Cu^{II}L^1M^{II}(H_2O)_3\}](ClO_4)_2$ (M = Co (3), M = Mn (4)). These two compounds were prepared in the same way as described below for **4** using the appropriate $M(ClO_4)_2\cdot 6H_2O$.

To a stirred suspension of **1** (0.218 g, 0.5 mmol) in methanol (15 mL) was added a methanol solution (5 mL) of $Mn(ClO_4)_2\cdot 6H_2O$ (0.127 g, 0.5 mmol). After a few minutes, the brown suspension changed to a red precipitate. This was dissolved by adding a requisite amount of acetonitrile. After 1 h of stirring, the solution was filtered and the filtrate was kept for slow evaporation. The diffraction quality red crystals that deposited over a period of few days were collected by filtration and washed with methanol.

(12) (a) Kahn, O. *Molecular Magnetism*; VCH Publications: New York, 1993; see also references therein. (b) Willett, R. D., Gatteschi, D., Kahn, O., Eds. *Magneto-Structural Correlations in Exchange Coupled Systems*; Kluwer Academic Publishers: Dordrecht, The Netherlands, 1985. (c) Amabilino, D. B.; Veciana, J. In *Magnetism*: *Molecules to Materials II*; Miller, J. S., Drillon, M., Eds.; Wiley-VCH: Weinheim, Germany, 2001. (d) Crawford, V. M.; Richardson, M. W.; Wasson, J. R.; Hodgson, D. J.; Hatfield, W. E. *Inorg. Chem.* **1976**, *15*, 2107. (e) Niemann, A.; Bossek, U.; Wieghardt, K.; Butzlaff, C.; Trautwein, A. X.; Nuber, B. *Angew. Chem. Int. Ed. Engl.* **1992**, *31*, 311. (f) Martin, D. S.; Bill, E.; Weyhermuller, T.; Bothe, E.; Weighardt, K. *J. Am. Chem. Soc.* **2005**, *127*, 6095. (g) Chlopek, K.; Bill, E.; Weighardt, T.; Weighardt, K. *Inorg. Chem.* **2005**, *44*, 7087. (h) Chen, P.; Root, D. E.; Campochiaro, C.; Fujisawa, K.; Solomon, E. I. *J. Am. Chem. Soc.* **2003**, *125*, 466. (i) Yoon, J.; Mirica, L. M.; Stack, T. D. P.; Solomon, E. I. *J. Am. Chem. Soc.* **2005**, *127*, 13680. (j) Brewer, G. A.; Sinn, E. *Inorg. Chem.* **1987**, *26*, 1529. (k) Birkelbach, F.; Winter, M.; Flörke, U.; Haupt, H.-J.; Butzlaff, C.; Lengen, M.; Bill, E.; Trautwein, A. X.; Wieghardt, K.; Chaudhuri, P. *Inorg. Chem.* **1994**, *33*, 3990. (l) Okawa, H.; Nishio, J. J.; Ohba, M.; Tadokoro, M.; Matsumoto, N.; Koikawa, M.; Kida, S.; Fanton, D. E. *Inorg. Chem.* **1993**, *32*, 2949. (m) Mohanta, S.; Nanda, K. K.; Thompson, L. K.; Flörke, U.; Nag, K. *Inorg. Chem.* **1998**, *37*, 1465. (n) Chou, Y.-C.; Huang, S.-F.; Koner, R.; Lee, G.-H.; Wang, Y.; Mohanta, S.; Wei, H.-H. *Inorg. Chem.* **2004**, *43*, 2759. (o) Mohanta, S.; Nanda, K. K.; Werner, R.; Haase, W.; Mukherjee, A.; Nag, K. *Inorg. Chem.* **1997**, *36*, 4656. (p) Mohanta, S.; Baitalik, S.; Dutta, S. K.; Adhikary, B. *Polyhedron* **1998**, *17*, 2669. (q) O'Connor, C. J.; Freyberg, D. P.; Sinn, E. *Inorg. Chem.* **1979**, *18*, 1077. (r) Leslie, K. A.; Drago, R. S.; Stucky, G. D.; Kitko, D. J.; Breese, J. A. *Inorg. Chem.* **1979**, *18*, 1885.

(13) König, E. *Magnetic Properties of Transition Metal Compounds*; Springer-Verlag: Berlin, 1966.

Table 1. Crystallographic Data of **1**−**4**

	1	**2**	**3**	**4**
empirical formula	$C_{20}H_{24}N_2O_5Cu$	$C_{60}H_{72}N_6Cl_2O_{23}Cu_4$	$C_{60}H_{72}N_6Cl_2O_{23}Cu_3Co$	$C_{60}H_{72}N_6Cl_2O_{23}Cu_3Mn$
fw	435.95	1570.30	1565.69	1561.70
crystal system	orthorhombic	monoclinic	monoclinic	monoclinic
space group	*Pbcn*	$P2_1/c$	$C2/c$	$C2/c$
a, Å	12.800(2)	22.1371(7)	15.4775(14)	15.551(10)
b, Å	19.804(4)	26.0705(8)	22.468(5)	22.630(9)
c, Å	7.660(3)	23.6500(7)	18.776(2)	18.964(4)
α, deg	90.00	90.00	90.00	90.00
β, deg	90.00	107.1423(8)	95.680(10)	95.55(5)
γ, deg	90.00	90.00	90.00	90.00
V, Å^3	1941.7(8)	13042.7(7)	6497.3(17)	6643(5)
Z	4	4	4	4
T, K	293(2)	295(2)	293(2)	293(2)
λ(Mo Kα), Å	0.71073	0.71073	0.71073	0.71073
$\rho_{calcd.}$, g cm^{-3}	1.491	1.599	1.601	1.562
μ, mm^{-1}	1.159	1.452	1.386	1.296
reflections collected	1714	117134	11754	6104
independent reflections	1713	29962	5695	5872
R_{int}	0.0258	0.0668	0.0067	0.0166
$R1^a$ ($I > 2\sigma(I)$)	0.0424	0.0538	0.0854	0.0570
w$R2^b$ (all data)	0.1180	0.1696	0.2106	0.1577

^{a} $R1 = [\sum||F_o| - |F_c||/\sum|F_o|]$. ^{b} $wR2 = [\sum w(F_o^2 - F_c^2)^2/\sum w(F_o^2)^2]^{1/2}$

Yield: 0.213 g (82%). Anal. Calcd for $C_{60}H_{72}N_6O_{23}Cl_2Cu_3Mn$: C, 46.14; H, 4.65; N, 5.38. Found: C, 46.04; H, 4.74; N, 5.28. IR (cm^{-1}, KBr): $\nu(H_2O)$, 3403m; ν(C═N), 1623s; $\nu(ClO_4)$, 1085vs, 618w.

Data for **3** follows. Yield: 0.201 g (77%). Anal. Calcd for $C_{60}H_{72}N_6O_{23}Cl_2Cu_3Co$: C, 46.03; H, 4.64; N, 5.37. Found: C, 46.16; H, 4.72; N, 5.28. IR (cm^{-1}, KBr): $\nu(H_2O)$, 3389w; ν(C═N), 1630s; $\nu(ClO_4)$,1088vs, 619w.

Crystal Structure Determination of 1−4. The crystallographic data of these compounds are summarized in Table 1. Diffraction data for **1** and **4** were collected on a Siemens P4 diffractometer, and a Bruker SMART charge-coupled device (CCD) diffractometer was used for **2**. In the case of **3**, data collection was made on a Bruker-Nonius FR-590 (MATH-3) diffractometer. All the data were collected in the $\omega - 2\theta$ scan mode using graphite-monochromated Mo Kα radiation having $\lambda = 0.71073$ Å. Three standard reflections were periodically monitored and showed no significant variation over data collection. The accurate unit cells were obtained by means of least-squares fits of 25 centered reflections. The intensity data were corrected for Lorentz and polarization effects, and semiempirical absorption corrections were made from ψ-scans. The structures were solved by direct and Fourier methods and refined by full-matrix least-squares methods based on F^2 with the programs SHELXS-97 and SHELXL-97.[14] Neutral atom scattering factors were taken from a standard source.[15] All non-hydrogen atoms were readily located and refined by anisotropic thermal parameters. The final least-squares refinements ($R1$) based on $I > 2\sigma(I)$ converged to 0.0424, 0.0538, 0.0854, and 0.0570 for **1**, **2**, **3**, and **4**, respectively.

Results and Discussion

Syntheses and Characterization. The mononuclear copper(II) complex $[Cu^{II}L^1{\subset}(H_2O)]$ (**1**) is readily obtained by reacting the ligand H_2L^1 with copper(II) acetate. As will be seen, the water molecule in **1** is not coordinated to the metal center, which remains in a square planar environment. The water molecule is hydrogen bonded to the phenolate oxygens and also to the oxygen atoms of the ethoxy side chains, resulting in the formation of an inclusion product.

Complex **1**, on reaction with copper(II) perchlorate, produces the tetranuclear copper(II) complex of the composition $[\{Cu^{II}L^1\}_2\{Cu^{II}L^1Cu^{II}(H_2O)_3\}](ClO_4)_2$ (**2**). Similarly, **1** smoothly reacts with the perchlorate salts of cobalt(II) and manganese(II) to produce the heterotetranuclear complexes of the composition $[\{Cu^{II}L^1\}_2\{Cu^{II}L^1M^{II}(H_2O)_3\}](ClO_4)_2$ (M^{II} = Co (**3**), M^{II} = Mn (**4**)). The variation in the ratio of the reactants **1** and $M(ClO_4)_2{\cdot}6H_2O$ (M = Cu, Co, or Mn) has no effect on the above-stated composition of the products. Surprisingly, it has not been possible to isolate an analogous nickel(II) complex. Nickel(II) perchlorate readily reacts with **1**, and from the resulting green solution, a product of the apparent composition $[\{Cu^{II}L^1\}_3\{Cu^{II}L^1Ni^{II}(H_2O)_3\}](ClO_4)_2$ has been obtained. However, as yet, we have not been able to obtain diffraction quality crystals to verify the composition.

The IR spectrum of the free ligand H_2L^1 exhibits two strong absorptions at 1627 and 1249 cm^{-1} due to $\nu_{C=N}$ and ν_{C-OEt} vibrations, respectively. In complex **1**, the vibrations due to $\nu_{C=N}$ (1620 cm^{-1}) and ν_{C-OEt} (1246 cm^{-1}) are slightly lowered in energies relative to the free ligand. Importantly, the IR spectrum of compound **1** exhibits two sharp bands at 3568 and 3518 cm^{-1} (Figure 1) in the region of water stretching. As will be seen, the water molecule in this compound is encapsulated in the O_4 compartment because of the formation of strong bifurcated hydrogen bonds with the phenoxo and ethoxy oxygens. In hydrated crystals, the asymmetric and symmetric ν_{O-H} stretching vibrations spread over a considerable range of energy and are normally observed as a broad band. However, because of encapsulation, the motion of the water molecule is so restricted in **1** that the asymmetric and symmetric stretchings appear separately. Similar separation of O−H stretching modes of vibration has been reported in a few oxovanadium(IV)

(14) (a) Sheldrick, G. M. *SHELXS-97*: *A Program for Crystal Structure Solution*; University of Göttingen: Göttingen, Germany, 1997. (b) Sheldrick, G. M. *SHELXL-97*: *A Program for Crystal Structure Refinement*; University of Göttingen: Göttingen, Germany, 1993.
(15) Cromer, D. T.; Waber, J. T. *International Tables for X-ray Crystallography*; The Kynoch Press: Birmingham, U.K., 1974; Vol. IV.

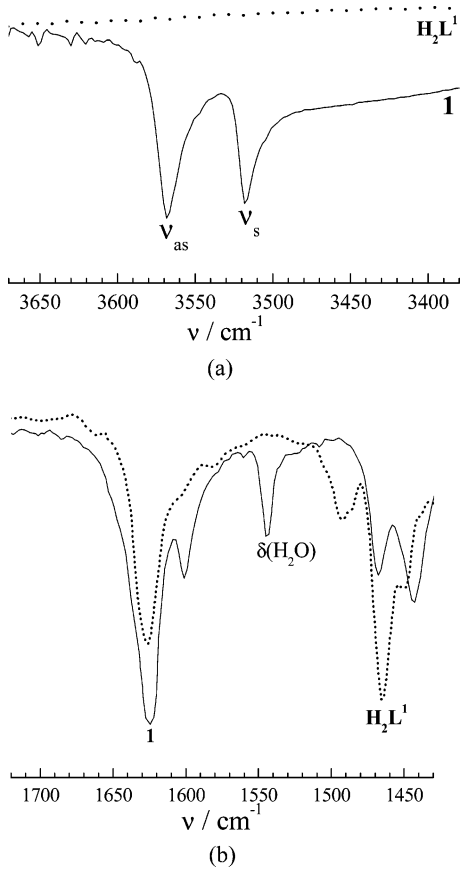

Figure 1. Part of the IR spectrum of H_2L^1 and $[Cu^{II}L^1(H_2O)]$ (**1**) demonstrating (a) stretching and (b) bending vibrations of the encapsulated water molecule in **1**.

compounds containing similar types of encapsulated water molecules.[9] The restricted motion of the water molecule is further evidenced in the occurrence of the bending mode of vibration at 1545 cm^{-1} (Figure 1).

In complexes **2**−**4**, the position of $\nu_{C=N}$ remains practically unchanged. Additionally, they exhibit the bands of the ionic perchlorate at ca. 1085 and 620 cm^{-1}. As compared to **1**, the band due to water stretching modes is broader in nature and observed in the range 3400−3340 cm^{-1}. It will be seen that in these compounds both encapsulated and nonencapsulated water molecules are present; therefore, the separation between asymmetric and symmetric stretching modes of vibration gets vitiated.

Description of the Structures of 1−4. The crystal structure of $[Cu^{II}L^1\subset(H_2O)]$ (**1**) is shown in Figure 2, and the selected bond lengths and angles are listed in Tables 2 and S1. The structure of **1** shows that it is a mononuclear compound having the metal center in the salen-type cavity of $[L^1]^{2-}$. As observed in related compounds, the Cu−N bond length (1.945(3) Å) is slightly longer than the Cu−O bond distance (1.911(2) Å).[10a,11] The N_2O_2 donors form a perfect plane, and the metal center lies exactly on this plane, adopting a square planar geometry. The *transoid* (177.19(11)°) and *cisoid* (83.8(2)−93.38(12)°) angles in the coordination environment of copper(II) deviate to a small extent from the ideal values. The water molecule in this compound is hydrogen bonded with the four oxygen atoms and is encapsulated in the acyclic O_4 compartment of $[L^1]^{2-}$. Each

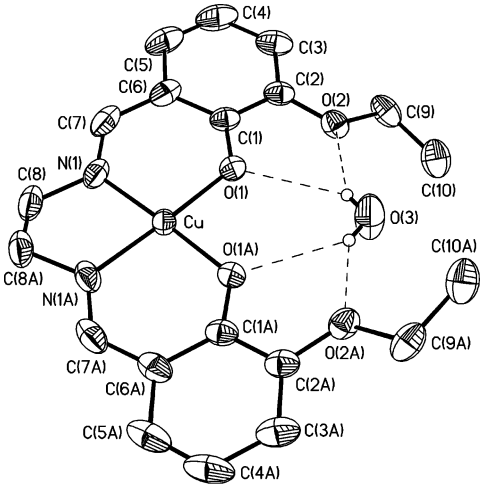

Figure 2. Crystal structure of $[Cu^{II}L^1\subset(H_2O)]$ (**1**).

Table 2. Selected Bond Lengths (Å) of **1**−**4**

compound	bond	distances (Å)	compound	bond	distances (Å)
1	Cu−N(1)	1.945(3)	**2** (Unit II)	Cu(6)−O(20)	1.885(3)
	Cu−O(1)	1.911(2)		Cu(7)−N(10)	1.933(4)
				Cu(7)−O(23)	1.902(3)
2 (unit I)	Cu(1)−O(4)	1.972(3)		Cu(7)−N(9)	1.946(4)
	Cu(1)−O(5)	2.374(3)		Cu(7)−O(24)	1.924(3)
	Cu(1)−O(1)	1.919(4)		Cu(8)−N(12)	1.933(4)
	Cu(1)−O(2)	1.961(3)		Cu(8)−O(27)	1.917(3)
	Cu(1)−O(3)	1.971(4)		Cu(8)−N(11)	1.925(4)
	Cu(2)−N(1)	1.926(4)		Cu(8)−O(28)	1.903(3)
	Cu(2)−O(5)	1.907(3)			
	Cu(2)−N(2)	1.914(4)	**3**	Co(1)−O(1)	2.124(6)
	Cu(2)−O(4)	1.917(3)		Co(1)−O(3)	2.047(11)
	Cu(3)−N(3)	1.926(5)		Co(1)−O(4)	2.059(7)
	Cu(3)−O(9)	1.890(3)		Cu(1)−N(1)	1.901(8)
	Cu(3)−N(4)	1.951(5)		Cu(1)−O(1)	1.885(6)
	Cu(3)−O(8)	1.915(4)		Cu(2)−N(2)	1.929(10)
	Cu(4)−N(6)	1.953(4)		Cu(2)−O(6)	1.892(7)
	Cu(4)−O(12)	1.933(3)		Cu(2)−N(3)	1.930(8)
	Cu(4)−N(5)	1.932(4)		Cu(2)−O(5)	1.886(7)
	Cu(4)−O(13)	1.897(3)			
			4	Mn(1)−O(1)	2.198(3)
2 (unit II)	Cu(5)−O(19)	2.055(3)		Mn(1)−O(3)	2.206(7)
	Cu(5)−O(20)	2.294(3)		Mn(1)−O(4)	2.150(4)
	Cu(5)−O(16)	1.977(3)		Cu(1)−N(1)	1.919(4)
	Cu(5)−O(17)	1.942(3)		Cu(1)−O(1)	1.893(3)
	Cu(5)−O(18)	1.948(3)		Cu(2)−N(2)	1.940(5)
	Cu(6)−N(8)	1.914(4)		Cu(2)−O(6)	1.904(4)
	Cu(6)−O(19)	1.910(3)		Cu(2)−N(3)	1.927(5)
	Cu(6)−N(7)	1.902(4)		Cu(2)−O(5)	1.895(4)

of the two water hydrogens forms bifurcated hydrogen bonds with one phenoxo and one ethoxy oxygen. The geometries of the hydrogen bonds are summarized in Table 3. The donor···acceptor contacts involving the phenoxo and ethoxy oxygens are 3.048 and 2.903 Å, respectively, indicating that the hydrogen bonds can be considered as moderately strong; those involving ethoxy oxygens are slightly stronger.

The structure of **2** consists of four perchlorate anions and two independent units of the tetracopper(II) dication of the composition $[\{Cu^{II}L^1\}_2\{Cu^{II}L^1Cu^{II}(H_2O)_3\}]^{2+}$. In each of the two independent units (unit I and unit II, Figure 3), the diphenoxo-bridged $[Cu^{II}L^1Cu^{II}(H_2O)_3]^{2+}$ cation is interlinked with two mononuclear $[Cu^{II}L^1]$ species by hydrogen bonding interactions (vide infra). In the dicopper(II) cores, one copper(II) ion occupies the N_2O_2 cavity, and the second

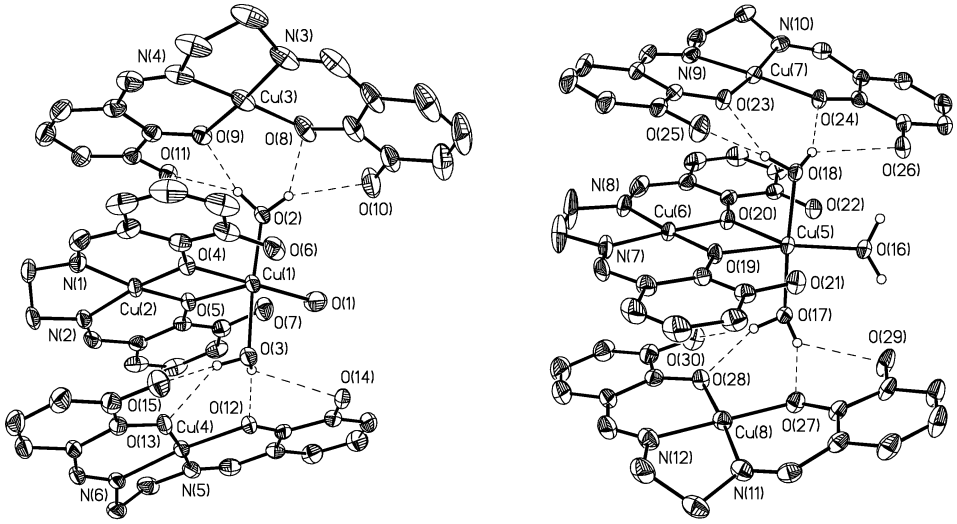

Figure 3. Structures of two tetracopper(II) units (units I and II) of composition $[\{Cu^{II}L^1\}_2\{Cu^{II}L^1Cu^{II}(H_2O)_3\}]^{2+}$, each containing one dinuclear $[Cu^{II}L^1Cu^{II}(H_2O)_3\}]^{2+}$ cation and two mononuclear $[Cu^{II}L^1]$ species, in **2**. Only those hydrogens participating in hydrogen bonds are shown. Except oxygens, other atoms of the ethoxy groups are also omitted for clarity.

Table 3. Geometries (Distances in Å and Angles in deg) of the Hydrogen Bonds Responsible for the Encapsulation of Water in **1**−**4**

compound	D−H···A/D···A	D···A	H···A	D−H···A
1	O(3)−H(31A)···O(1)	3.048	2.428	144.5
	O(3)−H(31)···O(2)	2.903	2.266	147.3
2	O(2)−H(2)···O(8)	2.839	2.095	140.4
	O(2)−H(2′)···O(9)	2.759	1.988	143.8
	O(2)−H(2)···O(10)	2.990	2.211	145.7
	O(2)−H(2′)···O(11)	3.005	2.257	141.2
	O(3)−H(3)···O(12)	2.755	1.932	151.8
	O(3)−H(3′)···O(13)	2.831	2.204	126.4
	O(3)−H(3)···O(14)	3.063	2.588	114.0
	O(3)−H(3′)···O(15)	2.982	2.142	155.2
	O(17)−H(17′)···O(27)	2.765	1.930	155.0
	O(17)−H(17)···O(28)	2.781	2.013	143.3
	O(17)−H(17′)···O(29)	2.977	2.351	127.2
	O(17)−H(17)···O(30)	3.099	2.336	143.7
	O(18)−H(18)···O(23)	2.740	2.046	134.1
	O(18)−H(18′)···O(24)	2.744	1.900	156.5
	O(18)−H(18)···O(25)	3.066	2.263	150.1
	O(18)−H(18′)···O(26)	2.999	2.376	126.7
3	O(4)···O(5A)	2.762		
	O(4)···O(6A)	2.809		
	O(4)···O(7A)	3.023		
	O(4)···O(8A)	2.927		
4	O(4)−H(41)···O(5)	2.813	2.094	143.9
	O(4)−H(42)···O(6)	2.853	2.229	131.6
	O(4)−H(41)···O(7)	3.051	2.342	142.8
	O(4)−H(42)···O(8)	2.956	2.190	152.9

compartment of $[L^1]^{2-}$ is occupied by another metal ion that is coordinated to the two bridging phenoxo oxygens and three water molecules. The ethoxy oxygens of the ligand remain uncoordinated.

The selected bond lengths and angles of the coordination environment of six copper(II) centers (Cu(2), Cu(3), Cu(4), Cu(6), Cu(7), and Cu(8)) in the N_2O_2 compartment are summarized in Tables 2 and S1. The Cu−N and Cu−O bond lengths lie in the ranges 1.902(4)−1.953(4) and 1.885(3)−1.933(3) Å, respectively. As in **1**, each of the Cu−N bond lengths are slightly longer than its respective trans Cu−O distance. The ranges of the *cisoid* (83.56(19)−96.01(17)°) and *transoid* (169.01(16)−177.27(17)°) angles, the average deviation (0.06−0.16 Å) of the donor atoms, and the displacement (0.007−0.025 Å) of the copper(II) center from the corresponding least-squares N_2O_2 plane indicate that the coordination environment of these metal ions deviates only to a small extent from the ideal values.

As already mentioned, in compound **2**, the second metal center (Cu(1) in unit I and Cu(5) in unit II) in the corresponding dinuclear units obtains a five-coordinate CuO_5 environment by the two bridging phenoxo and the three water oxygens. However, comparison of the relevant metric parameters in Table S2 indicates a significant difference between the coordination geometries of the O_5 environments of these two metal centers. In the case of Cu(1), the value of τ is 0.04, indicating an almost perfect square pyramidal geometry; the τ value is 0.37 in the case of Cu(5), indicating a considerably distorted square pyramidal geometry.[16] In the case of Cu(1), the square plane is defined by the O(1), O(2), O(3), and O(4) atoms and the phenoxo oxygen O(5) occupies the apical position. The metal atom lies almost on the least-squares plane (deviation only 0.02 Å). In contrast, Cu(5) is significantly displaced (0.22 Å) from the mean plane of the O(16), O(17), O(18), and O(19) atoms. In the equatorial O_4 square plane of Cu(1) and Cu(5), the Cu−O bond distances lie in the ranges 1.919(4)−1.972(3) and 1.942(3)−2.055(3) Å, respectively. By comparison, the apical Cu−O (phenoxo) bond distances are 2.374(3) Å for Cu(1) and 2.294(3) Å for Cu(5). The difference in the two dicopper(II) cores of unit I and unit II in compound **2** is also evidenced in their bridge angles [unit I, Cu(1)−O(5)−Cu(2) = 91.82(12)° and Cu(1)−O(4)−Cu(2) = 105.29(14)°; unit II, Cu(5)−O(20)−Cu(6) = 97.24(13)° and Cu(5)−O(19)−Cu(6) = 104.99(14)°] as well as in the dihedral angles (unit I, 77.4°; unit II, 87.2°) between the square planes of the two copper(II) centers. The Cu(1)···Cu(2) and Cu(5)···Cu(6) separations are 3.09 and 3.14 Å, respectively.

(16) Addison, W.; Rao, T. N.; Reedijk, J.; Rijn, J. V.; Verschoor, G. C. *J. Chem. Soc., Dalton Trans.* **1984**, 1549.

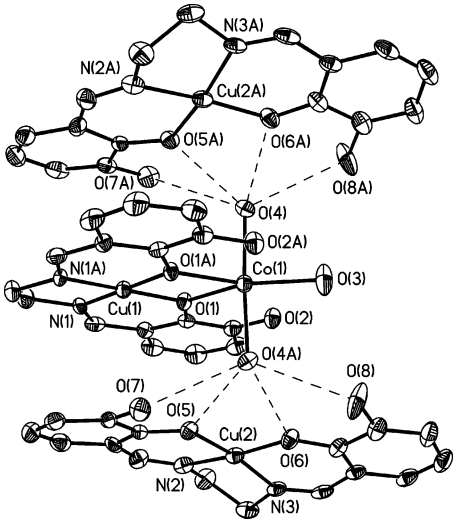

Figure 4. Structure of the tetrametal unit of composition $[\{Cu^{II}L^1\}_2\{Cu^{II}L^1Co^{II}(H_2O)_3\}]^{2+}$ consisting of one dinuclear $[Cu^{II}L^1Co^{II}(H_2O)_3]^{2+}$ cation and two mononuclear $[Cu^{II}L^1]$ species in **3**. Only those hydrogens participating in hydrogen bonds are shown. Except oxygens, other atoms of the ethoxy groups are also omitted for clarity.

Similar to that in **1**, water encapsulation through bifurcated hydrogen bonds occurs also in **2**. Among the three coordinated water molecules in units I and II, two are encapsulated in the O_4 cavity of two $[Cu^{II}L^1]$ species (Figure 3). In the case of unit I, $H_2O(2)$ is encapsulated in the O(8)O(9)O(10)O(11) compartment of the $[Cu^{II}(3)L^1]$ moiety, and $H_2O(3)$ is encapsulated in the O(12)O(13)O(14)O(15) compartment of the $[Cu^{II}(4)L^1]$ fragment. Similarly, in unit II, $H_2O(18)$ and $H_2O(17)$ interact with the $[Cu^{II}(7)L^1]$ and $[Cu^{II}(8)L^1]$ species, respectively. The geometries of the hydrogen bonds are summarized in Table 3. The O(water)···O(phenoxo) and O(water)···O(ethoxy) contacts lie in the ranges 2.74−2.83 and 2.97−3.10 Å, respectively, indicating that the hydrogen bonds can be considered as moderately strong in this case also. However, in contrast to **1**, in which the O(water)···O(phenoxo) distance is longer than the O(water)···O(ethoxy) contacts, the reverse is the case with **2**.

The structure of **3** consists of the heterotetranuclear $[\{Cu^{II}L^1\}_2\{Cu^{II}L^1Co^{II}(H_2O)_3\}]^{2+}$ cation (Figure 4) and two perchlorate anions. In **3**, similar to that in **2**, the dinuclear $[Cu^{II}L^1Co^{II}(H_2O)_3]^{2+}$ core is interlinked with two mononuclear $[Cu^{II}L^1]$ moieties by hydrogen bonding interactions. In this case, one-half of the molecule is symmetry related to the other half because of the presence of a crystallographic 2-fold axis. In the dinuclear $[Cu^{II}L^1Co^{II}(H_2O)_3]^{2+}$ core, the copper(II) ion occupies the N_2O_2 compartment, and the cobalt(II) center is pentacoordinated by the two phenoxo oxygens and three water molecules. In this case also, the ethoxy oxygens remain noncoordinated. The structural parameters in the square planar N_2O_2 coordination environment of the two crystallographically different copper(II) ions (Cu(1) and Cu(2)) are similar to those in compounds **1** and **2** (Tables 2 and S1).

The CoO_5 coordination environment (Figure 4, Tables 2 and S2) in **3** is highly distorted, and the extent of distortion is comparable with the CuO_5 environment in unit II of **2**. The value of τ in this case is 0.54, indicating that the geometry is intermediate between distorted square pyramidal and distorted trigonal bipyramidal.[16] In the case of a square pyramidal environment, either of the two phenoxo oxygens (O(1) and O(1A)) can be considered as the apical atom; the remaining oxygen atom between O(1) and O(1A) and the three water oxygens occupy the equatorial positions. The average deviations of O(1), O(3), O(4), and O(4A) from the least-squares O_4 plane is 0.31 Å, and the cobalt(II) center is displaced by 0.33 Å from this plane. For trigonal bipyramidal geometry, two phenoxo (O(1) and O(1A)) oxygens and one water (O(3)) oxygen define the equatorial plane; the two remaining water oxygens (O(4) and O(4A)) occupy the apical positions. The cobalt(II) ion lies on the equatorial O(1)-O(1A)O(3) plane. However, the O···O···O angles (O(1)···O(3)···O(1A) = 36.6°, O(3)···O(1)···O(1A) = 71.7°) in the equatorial plane are indicative of a high degree of distortion. The metal−ligand bond distances (Co(1)−O(1) = 2.124(6) Å) involving phenoxo oxygens are slightly longer than the bond lengths (Co(1)−O(3) = 2.047(11) Å, Co(1)−O(4) = 2.059(7) Å) involving the water oxygens. The Cu(1)−O(1)−Co(1) bridge angle and the Cu(1)···Co(1) distance in the dinuclear core are 102.6(3)° and 3.132 Å, respectively. As in **2**, the bridging moiety in the dinuclear core is highly twisted, as evidenced by the dihedral angles (91.7°) between the N_2O_2 square plane of the copper(II) center and the equatorial O_4 plane of the cobalt(II) environment.

The O_4 cavities of the two $[Cu^{II}L^1]$ moieties are occupied by two coordinated water molecules. In this case, two symmetry related water molecules ($H_2O(4)$ and $H_2O(4A)$) are hydrogen bonded with the oxygens of the two symmetry related $[Cu^{II}L^1]$ moieties, $[Cu^{II}(2A)L^1]$ and $[Cu^{II}(2)L^1]$, respectively. As the water hydrogens are not located, it is not possible to comment on the geometries of the hydrogen bonds. However, the O(water)···O(phenoxo) and O(water)···O(ethoxy) contacts (2.762−2.809 and 2.927−3.023 Å, respectively) are very similar to the corresponding distances in **2**, indicating the existence of similar types of bifurcated hydrogen bonds.

Compound **4** (Figure 5), which consists of the $[Cu^{II}L^1Mn^{II}(H_2O)_3]^{2+}$ cation and two $[Cu^{II}L^1]$ species, is isomorphous with **3**. The structural parameters of the coordination environment are summarized in Tables 2, S1, and S2, and the geometries of the hydrogen bonds are listed in Table 3. Because of the disorder of one coordinated water oxygen (O(3)) over two sites with equal occupancy, it is not possible to know the absolute values of some of the bond lengths and angles. However, taking one site (Figure 5, Tables 2 and S2) of the disordered oxygen, the nature of the coordination environment around manganese(II) can be understood. In this case, the value of τ is 0.49, indicating that, as in the cobalt(II) environment in **3**, the geometry around manganese(II) in **4** is highly distorted and intermediate between square pyramidal and trigonal bipyramidal.[16] In the dinuclear moiety, the Cu(1)−O(1)−Mn(1) bridge angle, Cu(1)···Mn(1) distance, and the dihedral angle between the square plane of the copper(II) ion and the O_4 plane of the manganese(II) ion are 103.78(15)°, 3.225 Å, and 91.2°, respectively. As in **3**, encapsulation of two coordinated water

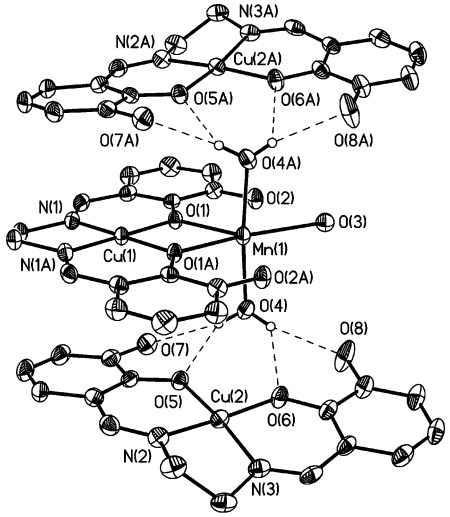

Figure 5. Structure of the tetrametal unit of composition $[\{Cu^{II}L^1\}_2\{Cu^{II}L^1\text{-}Mn^{II}(H_2O)_3\}]^{2+}$ consisting of one dinuclear $[Cu^{II}L^1Mn^{II}(H_2O)_3\}]^{2+}$ cation and two mononuclear $[Cu^{II}L^1]$ species in **4**. Only those hydrogens participating in hydrogen bonds are shown. Except oxygens, other atoms of the ethoxy groups are also omitted for clarity.

molecules takes place in the structure of **4** because the formation of bifurcated hydrogen bonds (Figure 5, Table 3).

Relative Extent of Water Encapsulation in 1−4. The relative extent of the encapsulation of water in **1**−**4** may be understood from the displacement of the water oxygen from the least-squares $O(phenoxo)_2O(ethoxy)_2$ plane. In the case of **1**, the oxygen atom of the encapsulated water lies on the least-squares $O(phenoxo)_2O(ethoxy)_2$ plane, and the oxygen atoms of the encapsulated water molecules in **2**−**4** are displaced by 0.92−1.23 Å from the corresponding $O(phenoxo)_2O(ethoxy)_2$ plane, indicating that the extent of encapsulation in **1** is much greater than that in the other compounds. It should be noted that treatment of compounds **2**−**4** with dimethylformamide results in the formation of compound **1**, indicating that the O_4 compartment is more preferable for water.

Resemblance of Water with Metal Ions. As mentioned earlier, interacting by the two phenoxo oxygens or by all the four oxygens, the O_4 compartment of $[L^1]^{2-}$ can accommodate 3d and 4f metal ions as well as water. Therefore, in this ligand system, encapsulation of water via hydrogen bonding interactions is very similar to the occupation of metal ions; the stabilization is achieved by electrostatic as well as by orbital overlap in the case of metal ions; in contrast, only the electrostatic interactions between water hydrogens and phenoxo or ethoxy oxygens are responsible for the inclusion of water. Moreover, both the formation of a bimetallic core from $[Cu^{II}L^1\subset(H_2O)]$ and the decomposition of the former to the latter by dimethylformamide resemble the transmetalation reaction.

Cocrystallization in 2−4. As discussed, the structures of **2**−**4** consist of one dinuclear $[Cu^{II}L^1M^{II}(H_2O)_3]^{2+}$ cation and two mononuclear $[Cu^{II}L^1]$ species. Clearly, compounds **2**−**4** are interesting examples of the cocrystal consisting of dinuclear and mononuclear moieties as the components. As the water molecule prefers to be encapsulated in the O_4 compartment, two of the coordinated water molecules interact with the mononuclear $[Cu^{II}L^1]$ species. Evidently, the tendency to encapsule the water molecule in the O_4 compartment of the mononuclear $[Cu^{II}L^1]$ moiety is the governing factor for the potential cocrystallization in **2**−**4**.

Magnetic Properties. The cryomagnetic behavior of **2** is shown in Figure 6 in terms of $\chi_M T$ versus T and χ_M versus T plots. The $\chi_M T$ value (1.53 $cm^3\ mol^{-1}$ K) at 300 K of **2** is very close to the theoretical value (1.50 $cm^3\ mol^{-1}$ K) for four isolated copper(II) ions with $g = 2$. On lowering of temperatures, $\chi_M T$ decreases very slowly to 1.43 $cm^3\ mol^{-1}$ K at 80 K. On further lowering of temperatures, $\chi_M T$ diminishes very rapidly to 0.59 $cm^3\ mol^{-1}$ K at 2 K. The profile indicates that there exists a weak antiferromagnetic interaction in this molecule. Although the metal ions in the dinuclear cores should interact with each other, the possibility of a magnetic exchange between the metal ion in the mononuclear species with the pentacoordinated metal center in the dinuclear cores should be discarded because these metal ions are separated as Cu(mononuclear)−O(phenoxo)···H−O(water)−Cu(pentacoordinated) and the Cu(pentacoordinated)···Cu(mononuclear) separations lie in the range 4.86−5.04 Å. Therefore, the two copper(II) centers in the $[Cu^{II}L^1]$ moieties should only influence the $\chi_M T$ values as a known amount of paramagnetic impurity. The rapid increase of the χ_M values at lower temperatures is indicative of such an assumption. Again, the absence of a maximum in the χ_M versus T plots is also indicative of the influence of the paramagnetic contribution of the two isolated $s = 1/2$ centers. As the structural parameters in the two dinuclear cores in **2** are significantly different, there should be two values of the exchange integral (J). However, consideration of two different J values for two different dinuclear cores is not possible because of the dependency of one J value on the other in the course of least-squares fitting. Considering average J values for the two dinuclear cores and the same value for the magnetic moment (μ_{Cu}) of the copper(II) centers in the mononuclear fragments, the theoretical expression for the molar magnetic susceptibility (χ_M) of a system of one exchange-coupled dicopper(II) and two mononuclear copper(II) moieties can be derived as[17a]

$$\chi_M = \frac{7.997\chi_D T + 2\mu_{Cu}{}^2}{7.997T} \qquad (1)$$

where

$$\chi_D = \frac{N\beta^2 g^2}{kT}\frac{2e^{2J/kT}}{1+3e^{2J/kT}}$$

Least-squares fitting of the experimental data with eq 1 leads to $J = -17.4\ cm^{-1}$, $g = 2.087$, and μ_{Cu} (fixed) = 1.73 BM;[17b] the agreement factor (R) defined as $[\sum\{(\chi_M T)_{obs} - (\chi_M T)_{calc}\}^2/\sum(\chi_M T)_{obs}{}^2]$ is 3.26×10^{-2}.

As shown in Figure 7, the $\chi_M T$ value (5.14 $cm^3\ mol^{-1}$ K) at 300 K of **4** is lower than the theoretical value (5.50 cm^3

(17) (a) $\chi_M = \chi_D + 2\chi_{Cu} = \chi_D + 2(\mu_{Cu}/2.828)^2/T$. (b) As the compounds **2**−**4** are isostructural, same μ_{Cu} value (1.73 BM) has been fixed in the simulation process.

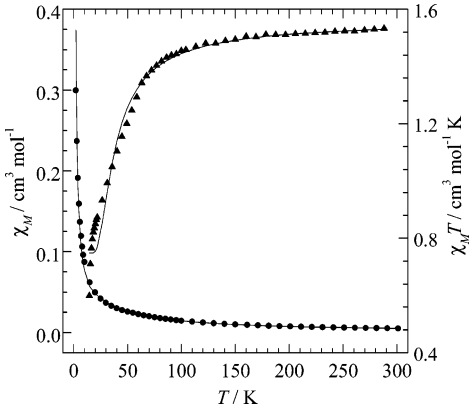

Figure 6. χ_M (circles) versus T and $\chi_M T$ (triangles) versus T plots for **2**. The solid lines represent the simulated curves.

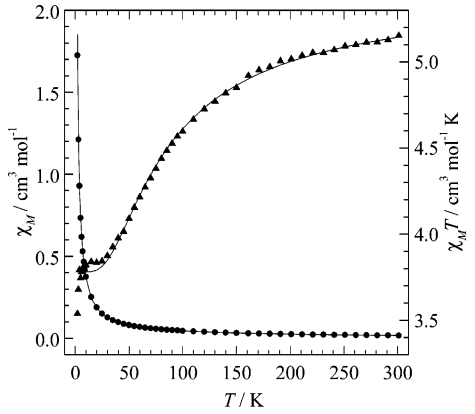

Figure 7. χ_M (circles) versus T and $\chi_M T$ (triangles) versus T plots for **4**. The solid lines represent the simulated curves.

mol^{-1} K) for the isolated one Mn^{II} ($s = 5/2$) and three Cu^{II} ($s = 1/2$) ions with $g = 2$. In this case, $\chi_M T$ gradually decreases on lowering of temperatures to reach a plateau (3.75 cm^3 mol^{-1} K) in the temperature range 25−10 K. Below 10 K, $\chi_M T$ decreases sharply to reach a value of 3.45 cm^3 mol^{-1} K at 2 K. Clearly, the nature of interaction between the copper(II) and manganese(II) centers in the dinuclear core is antiferromagnetic. The influence of the two noninteracting mononuclear copper(II) species can be evidenced from the absence of a maximum in the χ_M versus T plots as well as from the observation of a rapid increase in the χ_M values at lower temperatures (Figure 7). Considering one dinuclear $Cu^{II}Mn^{II}$ core and two noninteracting Cu^{II} centers, the theoretical equation of susceptibility can be derived as[17a]

$$\chi_M = \frac{7.997\chi_D T + 2\mu_{Cu}{}^2}{7.997T} \qquad (2)$$

where

$$\chi_D = \frac{N\beta^2 g^2}{kT}\frac{10 + 28e^{6J/kT}}{5 + 7e^{6J/kT}}$$

In this case, global minimization takes place with $J = -14$ cm^{-1}, $g = 1.985$, μ_{Cu} (fixed) = 1.73 BM, and $R = 1.02 \times 10^{-2}$.[17b]

The cryomagnetic behavior of **3** is shown in Figure 8. In this case, the $\chi_M T$ values are almost constant at ca. 3.73 cm^3 mol^{-1} K in the temperature range 300−110 K. Below 110 K, $\chi_M T$ decreases steadily to 0.96 cm^3 mol^{-1} K at 2 K. It may be noted that the magnetic behavior of **3** is additionally complicated due to the presence of first-order orbital angular momentum associated with the high spin cobalt(II) center. In comparison to the theoretical value (3.00 cm^3 mol^{-1} K), the high value (3.76 cm^3 mol^{-1} K) of $\chi_M T$ at 300 K of this compound is related to the orbital angular momentum of the cobalt(II) ion. It may also be mentioned that the isotropic model matches only poorly with the magnetic behavior of this compound (Supporting Information). Therefore, the susceptibility data have been simulated with eq 3,[12m,17a] which considers the exchange coupling between cobalt(II) and copper(II) centers in the dinuclear core, the single-ion zero-field parameter (D) of the cobalt(II) ion, and the contribution of the two isolated $s = 1/2$ spins. The simulation in this case is converged with $J = -8$ cm^{-1}, $g = 2.39$, $|D| = 2.9$ cm^{-1}, μ_{Cu} (fixed) = 1.73 BM, and $R = 2.32 \times 10^{-2}$.[17b]

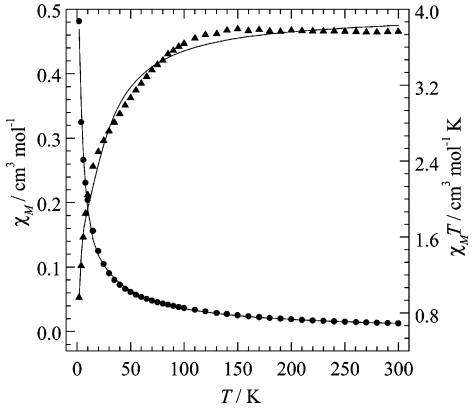

Figure 8. χ_M (circles) versus T and $\chi_M T$ (triangles) versus T plots for **3**. The solid lines represent the simulated curves.

$$\chi_M = \frac{7.997\chi_D T + 2\mu_{Cu}{}^2}{7.997T} \qquad (3)$$

where

$$\chi_D = \frac{2N\beta^2 g^2}{kT}\frac{e^A + 4e^C + e^E}{2e^A + e^B + e^D + e^E}$$

with

$$A = \left[4J + \frac{5}{4}D - (4J^2 - 2DJ + D^2)^{1/2}\right]/kT$$

$$B = \left[2J + \frac{1}{4}D\right]/kT$$

$$C = \left[6J + \frac{9}{4}D\right]/kT$$

$$D = \left[6J + \frac{1}{4}D\right]/kT$$

$$E = \left[\left(4J + \frac{5}{4}D\right) + (4J^2 - 2DJ + D^2)^{1/2}\right]/kT$$

As discussed, the bridging moieties of the dinuclear cores of **2** are highly distorted and unsymmetrical. In addition, there are two dinuclear cores with different extents of distortion.

Therefore, the established correlations[12a,d] in dialkoxo- and dihydroxo-bridged dicopper(II) systems cannot be extended in this case.[12q,r] However, the origin of the observed weak antiferromagnetic interaction ($J = -17.4$ cm^{-1}) in **2** can be understood from the relative orientation of the magnetic orbitals. The lobes of the $d_{x^2-y^2}$ orbital of Cu(1) or Cu(5) are directed only toward the equatorial phenoxo oxygen; the lobe of the d_{z^2} orbital is directed toward the apical phenoxo oxygen. As a matter of fact, only one phenoxo oxygen of both the dinuclear cores participates in the superexchange interaction, which, in turn, should result in a reduced antiferromagnetic interaction. Again, the Cu−O−Cu bridge angle (ca. 105°) involving the phenoxo oxygen participating in the exchange pathway is only slightly larger than the crossover angle (97°) proposed in the related systems.[12a,d] Evidently, the weak antiferromagnetic interaction between the metal centers in the dinuclear cores of **2** is related to the participation of only one bridging oxygen as well as the value (ca. 105°) of this bridge angle. It may be noted that a similar weak antiferromagnetic interaction ($J = -20$ cm^{-1}) has been observed previously in a similarly distorted dicopper(II) compound.[12r]

The exchange interaction between the metal centers in the $Cu^{II}Mn^{II}$ dinuclear core in **4** is also weakly antiferromagnetic ($J = -14$ cm^{-1}). In this case, the extent of interaction is a little less than that between the copper(II) centers in the dinuclear cores in **2**. In this compound, all the five d orbitals of manganese(II) are occupied by unpaired electrons. Although the $d_{x^2-y^2} \leftrightarrow d_{x^2-y^2}$ pathway gives rise to a antiferromagnetic interaction, the other four routes provide a ferromagnetic contribution to the overall magnetic coupling. These two opposite effects result in, in comparison to the coupling in the dicopper(II) cores in **2**, a reduction in the strength of the net antiferromagnetic interaction between the copper(II) and manganese(II) centers in **4**. However, the existence of an antiferromagnetic interaction in **4** is indicative that the $d_{x^2-y^2} \leftrightarrow d_{x^2-y^2}$ pathway still dominates the overall interaction.

Conclusions

The encapsulation of a water molecule in the vacant O_4 compartment of $[L^1]^{2-}$, resulting in the formation of the inclusion compound $[Cu^{II}L^1 \subset (H_2O)]$ (**1**), and the dinuclear−mononuclear cocrystals **2**−**4** are the major outcome of the present investigation. Although, there are a few examples of the encapsulation of water in similar O_4 compartments of oxovanadium(IV) and nickel(II) systems, $[Cu^{II}L^1 \subset (H_2O)]$ (**1**) is the first example of the inclusion compound of copper(II) derived from the related ligands. It may also be noted that, unlike in previously reported cocrystals of metal compounds, the governing factor for cocrystallization in the present investigation has been clearly understood in terms of hydrogen bonding interactions. Again, the role of water for potential cocrystallization of the metal ion species, as observed in **2**−**4**, or any other type of systems was not known previously. Therefore, the observation described here is interesting and it seems that other 3d−3d compounds derived from H_2L^1 and related ligands may be suitable to study inherent cocrystallization.

Acknowledgment. Financial support from the Department of Science and Technology, the Government of India (SR/S1/IC-27/2002), and the National Science Council, Taiwan (NSC-93-2113-M-032-002) is gratefully acknowledged. M.N. thanks CSIR, Government of India, for providing a fellowship.

Supporting Information Available: Crystallographic data in CIF format for compounds **1**−**4**, Tables S1 and S2, and the simulation of the susceptibility data of **3** with the isotropic model. These materials are available free of charge via the Internet at http://pubs.acs.org.

IC061049U